

REAL-TIME DYNAMIC IONOSPHERIC STORM MODELLING

Ljiljana R. Cander⁽¹⁾, Anna Belehaki⁽²⁾, Ioanna Tsagouri⁽²⁾

(1) Rutherford Appleton Laboratory, Chilton, Didcot, Oxon, OX11 0QX, United Kingdom, Email: l.cander@rl.ac.uk;

(2) National Observatory of Athens, Institute for Space Applications and Remote Sensing, Metaxa and Vas. Pavlou str. Palaia Penteli 15236, Greece, Email: belehaki@space.noa.gr; tsagouri@space.noa.gr

ABSTRACT

As radio communications systems become more technologically advanced, there is increasing demand to predict terrestrial plasma environment during severe space weather events. One important element of terrestrial plasma prediction is the onset of the ionospheric storms and their development during the first 24-hour. In the paper we discuss why a dynamic ionospheric storm forecast model, currently under developed, is needed and how it may be used to meet current and future radio communications as well as space weather operational requirements. At this stage, the model provides foF2 critical frequency of the F2 layer values during severe storm from disperse ionospheric and satellite observations. It makes use of the real-time ACE observations of the solar wind parameters to identify the storm onset and its intensity. Then the corrected model parameters are calculated at single stations and predictive accuracy is assessed. This work is expected to result in a real-time dynamic ionospheric storm model that has potential as part of an ionospheric/plasmaspheric specification and forecasting system within the COST271 Action and European space weather initiatives.

INTRODUCTION

Access to real-time information on ionospheric conditions over certain area (e.g. Europe), as a requirement for high frequency communication, satellite-to-ground links and solar-terrestrial research, has needed: (a) A network of vertical ionosondes involving as wide as possible to be set up for real-time data access [1]; (b) Short-term forecasting algorithms to be developed for foF2, M(3000)F2, TEC to predict their values up to 24 hours ahead [2, 3]; (c) A mapping algorithm for interpolation between the stations in the network to be implemented by using one of the available mapping procedure [4]; (d) Validation of the mapping and forecasting algorithms. As a response to these needs, an operational Short-Term Ionospheric Forecasting (STIF) tool for the European region based on continuous monitoring of the ionosphere has been developed and is available on the World Wide Web for interactive use (<http://ionosphere.rcru.rl.ac.uk/>) [5 and references therein]. It provides forecasting maps for up

to 24 hours ahead and archive measurement maps of the critical frequency of ionospheric F2 layer foF2, the Maximum Usable Frequency for a 3000 km range MUF(3000)F2, NeQuick modelled vertical total electron content (TEC) and Frequency of Optimum Traffic (FOT) for the area of interest at each UT hour. Similar technique can be applied at any other areas, as USA, Australia, China, where enough data are available in timely form.

Accuracy of forecast of foF2, MUF(3000)F2 and TEC has been studied through several statistical comparisons between measured and forecast values of foF2 and MUF(3000)F2. The forecast values selected were those deduced for one day ahead of the measured values. The principal results concern: (1) Comparisons at each UT hours during 10 geomagnetically quiet days of each month in two years of maximum solar activity in the current solar cycle 2000 and 2001; and (2) Comparisons at each UT hours during 5 geomagnetically disturbed days of each month in the same years. These gave the **Root Mean Square Error (RMSE)** of approximately 0.76 MHz for foF2 and 2.51 MHz for MUF(3000)F2 respectively and **Normalised RMSE** of 0.17 for both in the case of the geomagnetically quiet ionosphere.

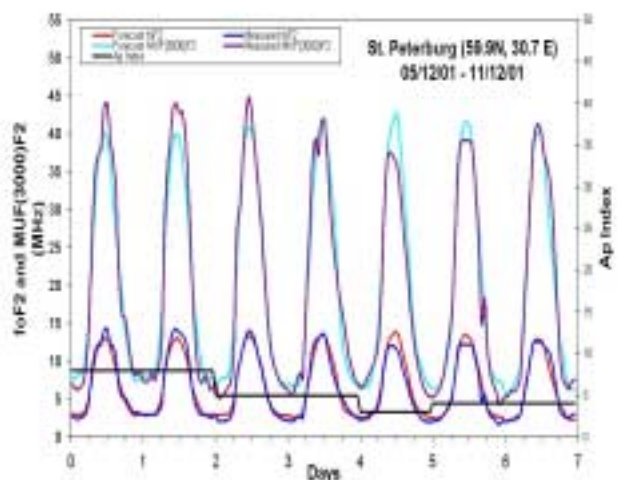


Fig.1. Comparison between measured and STIF forecast foF2 and MUF(3000)F2 values at St.Peterburg ionosonde station with Ap values as an indicator of the low geomagnetic activity

Fig. 1 shows an example of the typical **STIF** foF2 and MUF(3000)F2 results and measurements during seven quiet days of December 2001.

Global statistical comparisons for the 5 most disturbed days in 2000 and 2001 gave **RMSE** for foF2 and MUF(3000)F2 of 1.48 MHz and 4.38 MHz, respectively and **NRMSE**=0.67 for both. It should be noted that individual hourly RMSE in MUF(3000)F2 are generally about three times those of foF2. This is to be expected as M(3000)F2 propagation factors are typically about 3 though additional errors can be introduced by the measurements of the M(3000)F2 factor. Fig. 2 shows an example of the typical **STIF** foF2 and MUF(3000)F2 results and measurements during seven extremely disturbed days of March and April 2001.

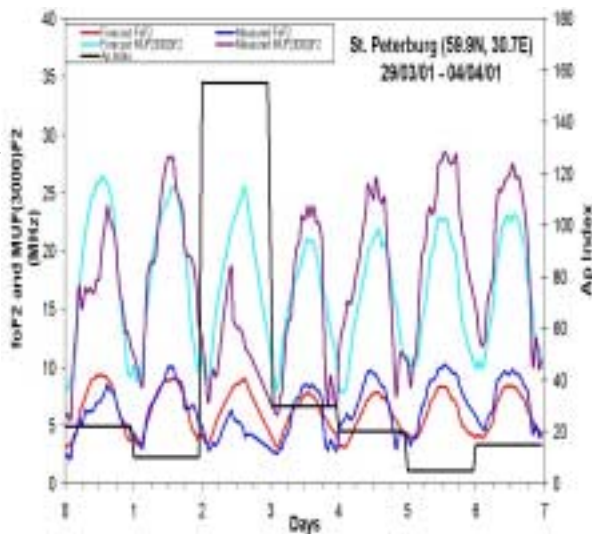


Fig. 2. Comparison between measured and **STIF** forecast foF2 and MUF(3000)F2 values at St. Peterburg ionosonde station with Ap values as an indicator of the high geomagnetic activity

These results clearly suggest that **STIF** tool is a very reliable forecasting technique in the relatively quiet geomagnetic conditions. Although these conditions prevail in the normal Earth's ionosphere, the conditions during the geomagnetic storms as these listed in Table 1 are of more importance for current and future radio communications services as well as space weather operational requirements and scientific studies.

Table 1 contains a list of major storms in the period September 1999 –November 2001 considered in this study with its primary goal of developing the understanding and the means to forecast how the ionospheric F2 layer will respond to abruptly and dramatically changing solar and geomagnetic conditions. It is an attempt to use the **Real-Time Solar Wind (RTSW)** data from the **Advanced Composition**

Explorer (ACE) spacecraft mission to derive criteria for issuing alerts for forthcoming major geomagnetic storms, as one of the dominant space weather events, and their effects on the ionospheric critical frequency foF2 in the first 24 hours. In the next Sections it will be shown how recent advances in real or near real-time observing and modelling systems that goal appears to be within reach.

Table 1. List of storms in the period September 1999 –November 2001 used in this study

Ri	Dst (nT)	START and MAIN DAYS
64	-149	22-23 September 1999
87	-231	21-22 October 1999
114	-169	11-12 February 2000
108	-321	06-07 April 2000
148	-317	15-16 July 2000
170	-235	12-13 August 2000
124	-201	17-18 September 2000
150	-182	4 -5 October 2000
205	-358	31 March-3 April 2001
115	-256	11-12 April 2001
140	-275	6-7 November 2001

THE EFFECT OF SOLAR WIND CONDITIONS IN IONOSPHERIC STORM DEVELOPMENT

One of the most popular and complete descriptions of the ionospheric storm-induced effects is the Prölss [6] phenomenological model, which was extended by Fuller-Rowell et al. [7,8]. This model captures most of the basic aspects of ionospheric storms, such the long-lived negative storm effects and daytime positive effects. Negative storm effects are attributed to the formation and evolution of the neutral composition bulge. The magnitude and the distribution of the negative ionospheric phase depend on the magnitude and the position of the neutral composition bulge. On the other hand, daytime positive effects are attributed to travelling atmospheric disturbances (TADs) launched by a sudden energy injection at auroral latitudes. Nevertheless, the prominent feature of large nighttime enhancements in the ionization density has yet to be explained and included in a new phenomenological model.

Recently, Belehaki and Tzagouri [9] in an investigation of the nighttime ionospheric response at middle latitudes under the light of the global solar wind-magnetosphere-ionosphere interaction suggested, that the recording of positive storm effects from ground ionosondes at night is strongly dependent first on the solar wind conditions leading to geomagnetic storms

and second on the intensity of the storm. Geomagnetic storms with initial phases, followed by short in duration but very fast evolving main phases, produce nighttime ionization depletion as a global effect at middle latitudes, independent of the storm intensity. During gradual driven storms, positive storm effects are frequently observed at middle to low latitudes. Given that geomagnetic storms are gradually evolving, the observation of positive effects at night depends also on the storm intensity and the latitude of the observation point.

The critical point in the explanation of the two different types of ionospheric response to different types of storms is the expansion of the neutral composition zone [9]. The sudden orientation of the IMF to very large southward field severely disturbs the magnetosphere-ionosphere system and changes the effective input energy to the auroral ionosphere, causing the very fast expansion of the deep negative phase equatorward. On the contrary, during gradually evolving storms the neutral composition disturbance zone remains restricted to high latitudes, and middle to low latitudes ionosphere allowed to be affected by other competing mechanisms.

In the light of these findings, one could argue that the forecast of the type of the storm and of storm intensity could lead to a prediction of the nighttime ionospheric response at middle latitudes. The crucial feature that determines the storm type is the arrival of a shock wave in the earth vicinity, which can be identified by the rate of change of B_z -IMF (dB_z/dt), the rate of change of solar wind number density (dn/dt), and the rate of change of solar wind bulk speed velocity (dU/dt). Another point of great importance is the rate of the solar wind energy entering the magnetosphere-ionosphere system, which is reflected in the rate of change of B_z -IMF.

The NASA Advanced Composition Explorer (ACE) spacecraft from the vantage L1 point performs measurements over a wide range of energies and nuclear masses, under all solar wind flow conditions, and during both large and small particle events including solar flares. The data are fundamental to enabling the formulation of highly accurate forecasting techniques and the subsequent issuance of alerts and warnings of incoming major geomagnetic disturbances and their possible effects on the structures in ionospheric layers variations [10]. The time delay for the solar wind to travel from the L1 point where ACE is to the Earth is about one hour, giving forecaster the advanced knowledge of the storm type one hour before its consequences are detectable in the Earth's environment. Therefore, the data from ACE could be a

useful tool in real time ionospheric space weather forecasting.

RESULTS

The analyses of the correlation between the ACE solar wind parameters and the ionospheric parameter foF2 for all storms shown in Table 1 was performed for number of days. Results are presented here only for an example of the impulse type of geomagnetic storm on

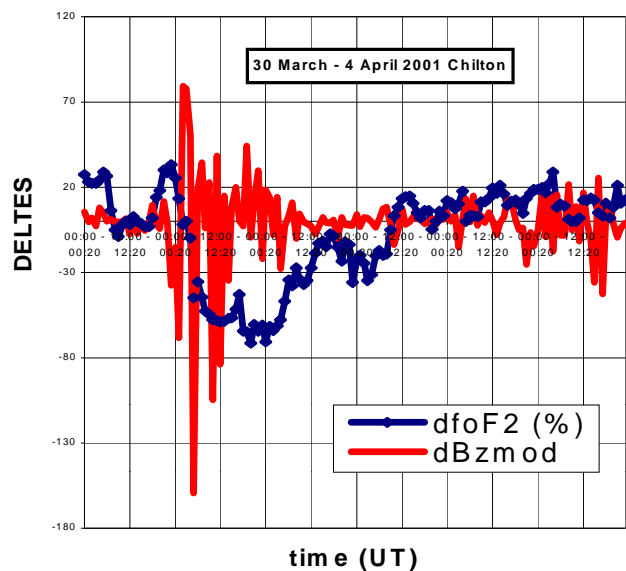


Fig. 3. B_z rate of change in 20 minutes interval with corresponding foF2 response for March 30, 2001 storm as seen at Chilton ionosonde station (51.5° N, -1.3° E).

30 March 2001 with initial compressive phase and very fast evolving main phase, triggered by an interplanetary shock wave in Fig. 3 and an example of the gradual type of geomagnetic storm on 3 October 2000 with no initial phase, with slowly evolving main phase, driven by gradual reversal of B_z -IMF to weak southward magnetic field in Fig. 4, respectively. These results generally reveal a unique opportunity to predict the F2 layer response to geomagnetic storm by using the ACE data in near real time mode.

Fig. 3 shows that the F2 layer ionization expressed in percentage deviation of hourly foF2 from median values, $dfoF2$ (%), immediate response of the B_z expressed by $dBzmod$ parameter ($dBzmod=100*dBz/dt$). Minutes after $dBzmod$ changes from +70 to -100, the $dfoF2$ (%) revealed a huge negative response of more than 50% followed by future decrease up to -70% during the main phase of the storm. The negative storm effect over Chilton was dominant for more than 36 hours. The October 2000 storm develops in two steps, with its first intensification observed on October 3, and the

second one the next day. Both storm intensifications are triggered by gradual changes in Bz also caused ionization depletion in the F region. Although, the plots differ significantly in details, as depicted in Fig. 4, the sudden changes in the dBzmod are always followed by negative storm effects that can be quantified.

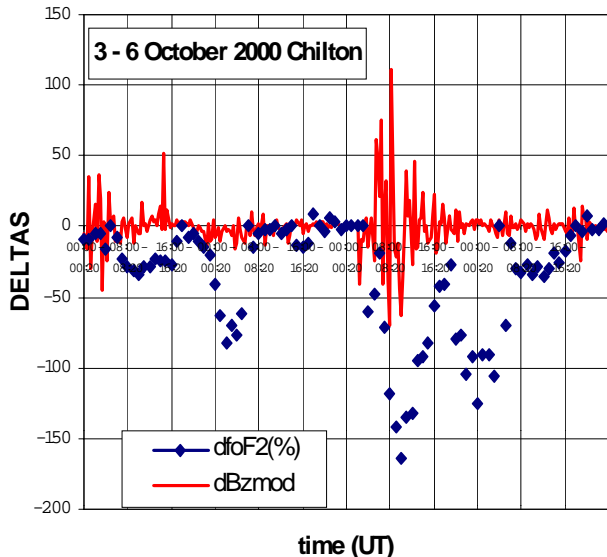


Fig. 4. Bz rate of change in 20 minutes interval with corresponding foF2 response for October 3, 2000 storm as seen at Chilton ionosonde station (51.5° N, -1.3° E).

DISCUSSION AND CONCLUSIONS

The ionospheric critical frequency of the F2 layer is highly variable on time-scales ranging from decades to seconds with the occurrence of ionospheric disturbances associated with geomagnetic storms. Many attempts have been made recently in Europe to study the space environmental disturbances frequently referred to as space weather [5]. In these studies the focus is on forecasting the geomagnetic storm effect on main ionospheric parameters to enable extreme conditions to be quantified so that particularly for telecommunications planning likely variability bounds can be defined. In general, forecasts are made mostly on the basis of persistence and recurrence that are not always strong. Current 24 hour forecasting service (<http://ionosphere.rcru.rl.ac.uk/>) relies heavily on an extrapolation of past and prevailing ionospheric conditions. In practice this requires an automation of the data gathering and processing and on-line forecasting message distribution.

There has been ample evidence from different national as well as international space weather research projects that true forecasts of ionospheric disturbances are needed with lead times of up to 24-hours of the present. Very recently sufficient real-time data on interplanetary conditions (e.g. solar-wind parameters)

have been obtained to do this effectively [11]. However, F-region storm morphology has such a complex spatial and temporal structure that requires continuous monitoring of the high resolution. In this paper we examine the solar-terrestrial conditions and ionospheric F2 layer responses surrounding two geomagnetic storms in 23 solar cycle to illustrate what knowledge is required to the build up of the successful real-time dynamic ionospheric storm forecasting algorithm. The implementation of this algorithm is currently in progress.

REFERENCES

1. Hanbaba R., Improved quality of service in ionospheric telecommunication systems planning and operation, *COST Action 251 Final Report*, Space Research Centre, Warsaw, 1999.
2. Kutiev I., P. Muhtarov, Lj. R. Cander, M. Levy, Short-term prediction of ionospheric parameters based on autocorrelation analysis, *Annali di Geofis.*, 42(1), 121, 1999.
3. Hochegger, G., B. Nava, S. Radicella and R. Leitinger, A family of ionospheric models for different uses, *Phys. Chem. Earth (C)*, 25, 307, 2000.
4. Samardjiev, T., P.A. Bradley, Lj.R. Cander, and M.I. Dick, Ionospheric mapping by computer contouring techniques, *Electronics Lett.*, 29(20), 1794, 1993.
5. Cander, Lj.R., Toward forecasting and mapping ionospheric space weather under the COST actions, *Adv. in Space Res.*, in press, 2003.
6. Prölss, G.W., On explaining the local time variation of ionospheric storm effects, *Ann. Geophys.*, 11, 1-9, 1993
7. Fuller-Rowell, T.J., M.V. Codrescu, R.J. Moffett and S. Quegan, Response of the thermosphere and ionosphere to geomagnetic storms, *J. Geophys. Res.*, 99, 3893, 1994.
8. Fuller-Rowell T.J., M.V. Codrescu, H. Rishbeth, R.J. Moffett and S. Quegan, On the seasonal response of the thermosphere and ionosphere to geomagnetic storms, *J. Geophys. Res.*, 101, 2343, 1996.
9. Belehaki A. and I. Tsagouri, On the occurrence of storm induced nighttime ionisation enhancements at ionospheric middle latitudes, *J. Geophys. Res.*, 107, 8, 2002.
10. Kappenman, J. G., Geomagnetic storm forecasting mitigates power system impacts, *IEEE Power Engineering review*, 18, N.11, 1998.
11. Kamide, Y., From discovery to prediction of magnetospheric processes, *J. Atmos. Sol-Terr. Phys.*, 62, 1659-1668, 2000.